



TITLE:

Screw dislocation-induced growth spirals as emissive exciton localization centers in Al-rich AlGa_N/AlN quantum wells

AUTHOR(S):

Funato, Mitsuru; Banal, Ryan G.; Kawakami, Yoichi

CITATION:

Funato, Mitsuru ...[et al]. Screw dislocation-induced growth spirals as emissive exciton localization centers in Al-rich AlGa_N/AlN quantum wells. AIP Advances 2015, 5(11): 117115.

ISSUE DATE:

2015-11-06

URL:

<http://hdl.handle.net/2433/207642>

RIGHT:

© 2015 Author(s). All article content, except where otherwise noted, is licensed under a Creative Commons Attribution 3.0 Unported License.



Screw dislocation-induced growth spirals as emissive exciton localization centers in Al-rich AlGaN/AlN quantum wells

Mitsuru Funato, Ryan G. Banal, and Yoichi Kawakami

Citation: *AIP Advances* **5**, 117115 (2015); doi: 10.1063/1.4935567

View online: <http://dx.doi.org/10.1063/1.4935567>

View Table of Contents: <http://scitation.aip.org/content/aip/journal/adva/5/11?ver=pdfcov>

Published by the *AIP Publishing*

Articles you may be interested in

Emission mechanisms in Al-rich AlGaN/AlN quantum wells assessed by excitation power dependent photoluminescence spectroscopy

J. Appl. Phys. **117**, 075701 (2015); 10.1063/1.4908282

Excitonic localization in AlN-rich $\text{Al}_x\text{Ga}_{1-x}\text{N}/\text{Al}_y\text{Ga}_{1-y}\text{N}$ multi-quantum-well grain boundaries

Appl. Phys. Lett. **105**, 122111 (2014); 10.1063/1.4896681

Optical gain characteristics in Al-rich AlGaN/AlN quantum wells

Appl. Phys. Lett. **104**, 181102 (2014); 10.1063/1.4875592

Modulating optical polarization properties of Al-rich AlGaN/AlN quantum well by controlling wavefunction overlap

Appl. Phys. Lett. **103**, 181117 (2013); 10.1063/1.4828667

Edge and screw dislocations as nonradiative centers in InGaN/GaN quantum well luminescence

Appl. Phys. Lett. **78**, 2691 (2001); 10.1063/1.1369610



NEW Special Topic Sections

NOW ONLINE

Lithium Niobate Properties and Applications:
Reviews of Emerging Trends

AIP | Applied Physics
Reviews



Screw dislocation-induced growth spirals as emissive exciton localization centers in Al-rich AlGaIn/AlN quantum wells

Mitsuru Funato,^a Ryan G. Banal,^b and Yoichi Kawakami

Department of Electronic Science and Engineering, Kyoto University, Kyoto 615-8510, Japan

(Received 17 June 2015; accepted 30 October 2015; published online 6 November 2015)

Screw dislocations in Al-rich AlGaIn/AlN quantum wells cause growth spirals with an enhanced Ga incorporation, which create potential minima. Although screw dislocations and their surrounding potential minima suggest non-radiative recombination processes within growth spirals, in reality, screw dislocations are not major non-radiative sinks for carriers. Consequently, carriers localized within growth spirals recombine radiatively without being captured by non-radiative recombination centers, resulting in intense emissions from growth spirals. © 2015 Author(s). All article content, except where otherwise noted, is licensed under a Creative Commons Attribution 3.0 Unported License. [<http://dx.doi.org/10.1063/1.4935567>]

Nitride semiconductors are indispensable in optical devices such as light-emitting diodes (LEDs) and laser diodes. One of their most interesting characteristics is related to threading dislocations. Although LEDs are typically grown on sapphire substrates and involve numerous threading dislocations, their external quantum efficiency exceeds 80% in the blue spectral range.¹ To clarify the cause of this apparent contradiction, the impact of threading dislocations on the local emission inhomogeneity of InGaIn violet to visible light emitters has extensively been studied.^{2–9} It has been demonstrated that threading screw, mixed, and edge dislocations act as non-radiative recombination centers, but the influence on the reduction of the emission intensity depends on the type of dislocation.

Screw dislocations in InGaIn often form growth spirals, which have a higher In composition.^{2,3,9} (The formation mechanism of growth spirals can be explained by the Burton-Cabrera-Frank (BCF) crystal growth theory; dislocations create steps on the surface, which avert the propagation of monolayer steps that originate from the crystal tilt and result in growth spirals.¹⁰) Because a higher In composition lowers the potential energy, it is reasonable to consider that carriers within growth spirals are eventually captured by screw dislocations. However, the literature is unclear. For example, Refs. 2 and 9 contradict each other and have suggested that the emissions around growth spirals are enhanced and suppressed, respectively. Because both studies use InGaIn films without quantum confinement, the effect of the potential barrier due to thinner quantum wells (QWs) near screw dislocations⁶ is exclusive. In this respect, it is interesting to note that the electrical activity of screw dislocations in GaIn depends on the core structure, and there is a core configuration that does not create a gap state.¹¹ Thus, the role of screw dislocations remains debatable even for a rather mature material like InGaIn.

For Al-rich AlGaIn, which is an emerging material for deep ultraviolet light emitters and detectors, macroscopic studies have examined the correlation between the x-ray diffraction line width (*i.e.*, dislocation density) and the emission intensity.^{12,13} Although the non-radiative nature of edge dislocations has been suggested, the micro or nanoscopic influences of dislocations on the optical properties of Al-rich AlGaIn have yet to be elucidated regardless of the dislocation type. In this study, we experimentally investigate the roles of screw dislocations and the resultant growth spirals in Al-rich AlGaIn QWs.

^aCorresponding author: funato@kuee.kyoto-u.ac.jp

^bPresent address: Optical and Electronic Materials Unit, National Institute for Materials Science (NIMS), 1-1 Namiki, Tsukuba, Ibaraki 305-0044, Japan



The samples were grown on sapphire (0001) substrates by metalorganic vapor phase epitaxy at a growth pressure of 76 Torr in a H_2 ambient. The source precursors were trimethylaluminum, trimethylgallium, and ammonia. Prior to AlN growth, the sapphire substrate was subjected to the nitridation process with ammonia,¹⁴ which was initiated at 1000 °C and continued up to the growth temperature of AlN (1200 °C) (case b in Ref. 14). Then 2.3- μm -thick AlN was grown. As discussed in Ref. 14, AlN is Al polar, and nitridation of sapphire prevents cracks from being induced due to void formation within the film. In addition, the surface morphology of AlN exhibits dislocations at the surface, which may be the precursor for step-flow growth by growth spirals. Finally a 1.5-nm-thick $\text{Al}_{0.8}\text{Ga}_{0.2}\text{N}$ single QW (SQW) covered with a 15-nm-thick AlN cap layer was grown at 1140 °C.

Figure 1 displays atomic force microscopy (AFM) images of the SQW surface. The monolayer steps and atomically flat terraces indicate step-flow growth. In addition, growth spirals¹⁰ are observed. The growth spirals are not a single continuous type, but can be classified into two different types: A and B. Type A, which is less common, is a spiral system that forms a lot of branches. As shown by the solid outline in Fig. 1, type A occurs around a large dislocation core (*e.g.*, a nanopit). In contrast, the more common type B is composed of two interlacing components rotated by 180°.

The rotation in type B is attributed to the lateral growth anisotropy due to different crystallographic orientations. A similar structure has been reported for GaN,^{15–17} and its origin is attributed to screw dislocations; to compensate for the Burgers vector of screw dislocations ($\pm c$), two interlacing spiral components with monolayer steps ($= c/2$) must co-exist. Likewise, because the estimated areal density of the spirals in our AlGa_{0.2}N ($6 \times 10^8/\text{cm}^2$) is comparable to the screw dislocation density estimated from the x-ray diffraction line width ($4 \times 10^8/\text{cm}^2$), the observed spirals most likely originate from screw dislocations.

It is interesting to note that many spirals group into pairs, as shown in the magnified image of Fig. 1. Similar spiral pairs where two spirals grow in the same counterclockwise direction have been observed in GaN, and the estimated total Burgers vector is $2c$.¹⁵ However, the spiral pairs in our Al-rich AlGa_{0.2}N do not necessarily have the same sign. The spiral pairs on the right hand side of the magnified image of Fig. 1 grow counterclockwise with the same sign, and they tend to reinforce each other. On the other hand, those on the left hand side exhibit opposing growth directions with the opposite signs,

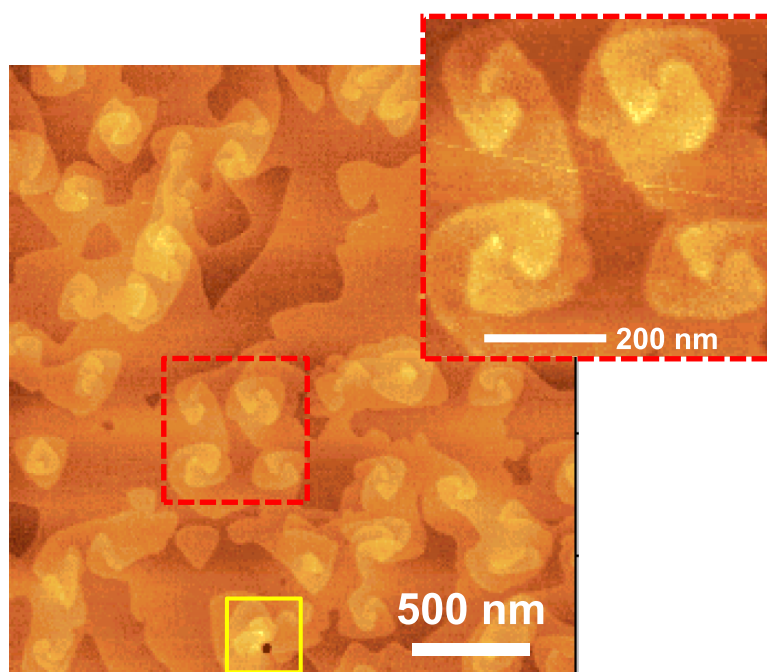


FIG. 1. AFM image of the AlGa_{0.2}N SQW. Magnified image indicates pairs of typical growth spirals (type B). Solid (yellow) outline indicates another minor spiral (type A) formed around a nanopit.

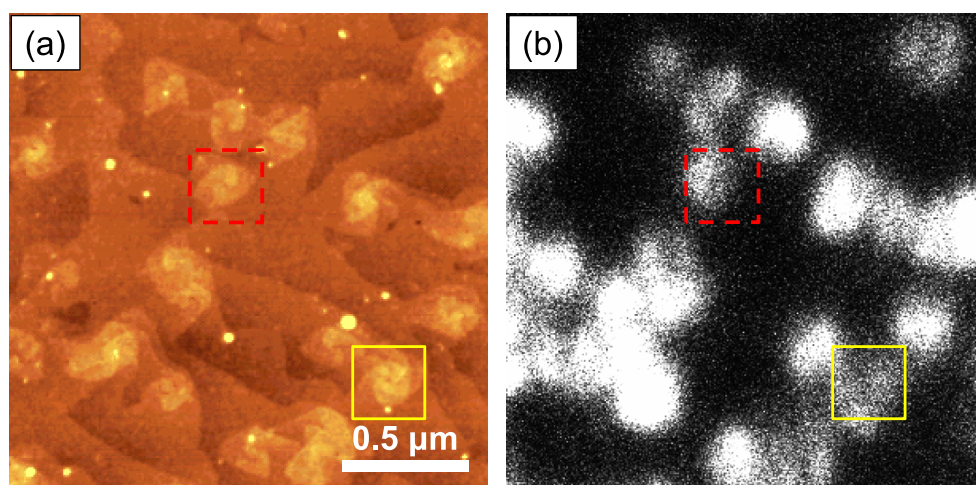


FIG. 2. (a) AFM image and (b) panchromatic CL intensity map of the AlGaIn/AlIn SQW acquired at RT. Solid (yellow) and broken (red) outlines represent type A and B spirals, respectively.

and they tend to annihilate each other. The structure of the dislocation pairs is presumably determined by the position where two dislocations cut the surface. For spiral pairs with opposite signs, the total Burgers vector is zero, and the pair screw dislocations cut the same atomically flat surface.

A growth spiral can continue to sweep around the crystal's surface as long as it does not encounter a surface barrier (*e.g.*, a dislocation or another spiral). Areas far from the growth spirals have wider terrace widths than those within a growth spiral (Fig. 1). It has been reported that the terrace width of a growth spiral is related to the degree of supersaturation.^{10,16,17} Assuming that the degree of supersaturation is uniform, a wider terrace width may be related to the off-cut angle of the substrate.

The spatially resolved optical properties were assessed by cathodoluminescence (CL) at room temperature (RT). Figure 2 compares an AFM image with a panchromatic CL intensity map taken at the same position. Interestingly, both types of growth spirals have stronger emissions than their surroundings, and the screw dislocations are not visible as dark spots. Although the reason for the latter is unclear, it is noteworthy that a certain core configuration does not contribute to non-radiative recombination, as described in the introduction.¹¹ The origin of the bright emissions around the growth spirals is discussed below.

Three-dimensional structures can improve light extraction because the total reflection is suppressed. This phenomenon is often utilized in the case of a patterned sapphire substrate¹⁸ or a three-dimensional light emitter.^{19,20} However, such a structural effect can be excluded in this study because the growth spirals (Fig. 1) have vertical dimensions of a few monolayers, which are much smaller than the wavelength of interest. Instead, the improved internal quantum efficiency should account for the origin of the observed CL bright spots.

Figure 3 displays the CL spectra of the AlGaIn SQW at RT. The inset is a panchromatic CL intensity map, where the averaged CL spectrum is acquired. The spatially resolved CL spectrum taken at a bright spot (green circle in the inset) is located at a lower energy than that at a dark spot (blue circle). Measurements at different positions confirm this tendency. Furthermore, the peak energy of the CL spectrum at the bright spot is nearly the same as that of the averaged CL spectrum, indicating that the emission from bright spots (*i.e.*, growth spirals) dominates the macroscopic luminescence properties. These findings indicate that potential minima form at growth spirals where captured carriers more efficiently recombine radiatively.

Because our sample is an AlGaIn SQW, the well-width and Al-compositional fluctuations may be responsible for the potential minima. To distinguish between these two, scanning transmission electron microscopy (STEM) was performed. The specimen was prepared by focused ion beam etching. The acceleration voltage for TEM observations was 200 kV. Figure 4(a) shows a STEM high-angle annular dark-field (HAADF) image of the sample (11 $\bar{2}$ 0) cross section. The horizontal bright contrast

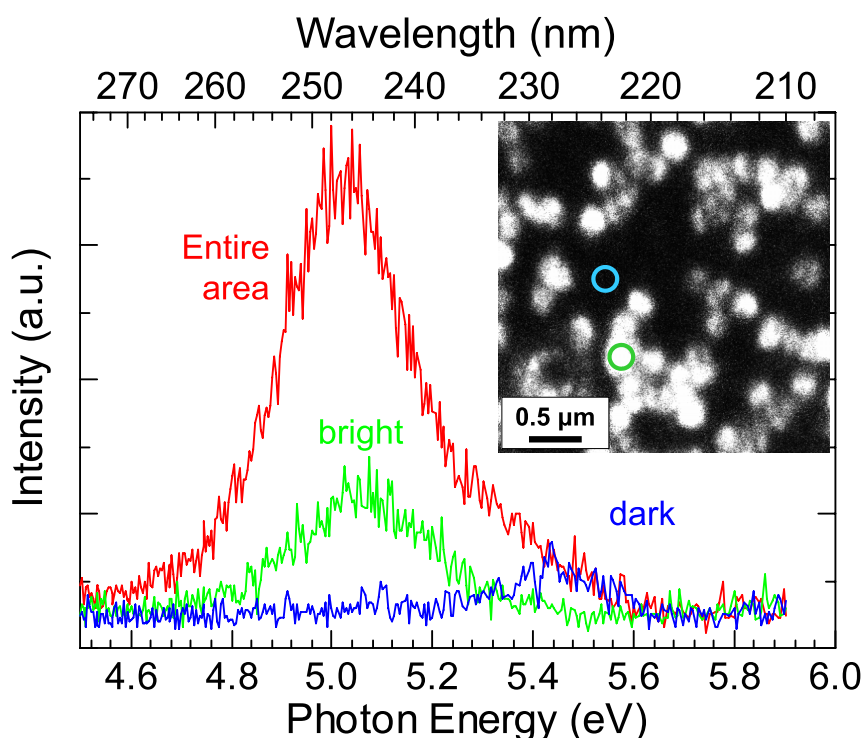


FIG. 3. CL spectrum averaged over the entire area of the inset CL panchromatic image and those acquired at a bright spot (green circle in the inset) and a dark spot (light blue circle). Bright spots correspond to growth spirals.

(AA') is due to the AlGa_N SQW, while the nearly vertical bright contrast is due to a well-isolated threading dislocation running from the underlying AlN to the surface. Based on the invisibility conditions revealed by TEM, the dislocation is a screw dislocation. Generally, scattering of an irradiated electron beam within a material causes a bright contrast in STEM-HAADF, which is why AlGa_N containing heavier atoms (Ga) and dislocations exhibit bright contrasts. (The former is the so-called Z-contrast.)

Figure 4(a) indicates that the screw dislocation in the present AlGa_N SQW is not accompanied by a V-pit.^{6,21,22} (Note that typical V-pits composed of the {11 $\bar{0}$ 1} planes should clearly be observed when viewed along the [11 $\bar{2}$ 0] direction, as in the case of this study.) Figure 1 confirms the absence of V-pits on the AlGa_N surface. Therefore, semipolar narrow QWs around V-pits, which act as potential barriers that prevent carriers from being captured in screw dislocations,^{6,22} do not exist in our AlGa_N SQWs. Consequently, such potential barriers cannot be responsible for the invisibility of screw dislocations in the CL maps (Fig. 2). To clarify the cause of the invisibility, a further investigation is necessary.

To separately estimate the contrast variation due to the Al composition or dislocations, the line profiles along AA' and BB', which are defined in Fig. 4(a), are plotted in Fig. 4(b). Line BB' is located just beneath the QW (AA'). As expected, the screw dislocation shows a bright contrast in both profiles. Comparing the AA' and BB' line profiles reveals that profile AA' involves an additional factor to brighten the contrast. Because the well width is independent of the position, the additional factor is presumed to be a higher Ga composition. The lateral dimensions support this assertion; the brighter contrast region spans ~250 nm (from 150 to 400 nm) in Fig. 4(b), which agrees well with the growth spiral dimensions shown in Figs. 1 and 2. In addition, previous papers have suggested that more Ga atoms are accumulated at the macro or bunched steps on the AlGa_N surface.^{23–26} Although growth spirals on AlGa_N are not composed of bunched steps, the step density around them is much higher than those on terraces. Therefore, the circumstances for adatoms at the growth spirals may resemble those at bunched steps, which may promote Ga incorporation at the growth spirals. These findings

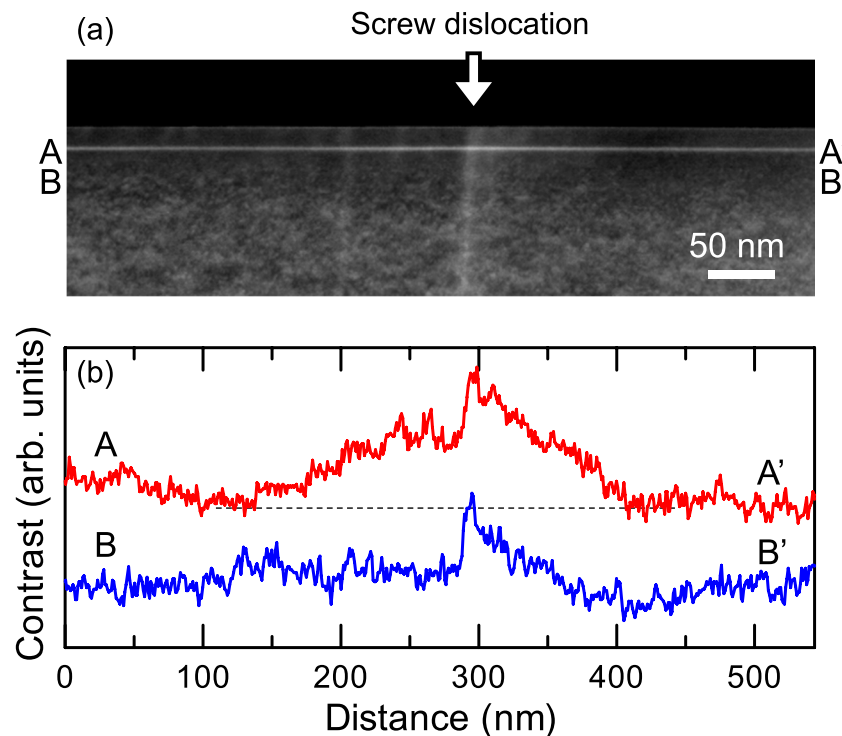


FIG. 4. (a) Cross sectional STEM-HAADF image of the AlGaIn SQW taken along the $[11\bar{2}0]$ zone axis. (b) Line profiles of the STEM-HAADF contrast along AA' and BB' defined in (a). Dotted line indicates the background contrast for AA'.

lead us to conclude that the growth spirals in AlGaIn QWs involve more Ga to form potential minima, which act as emissive localization centers.

To summarize, we demonstrate that the growth spirals possess a higher Ga composition compared with the surrounding region and form potential minima. Despite of the presence of screw dislocations, the potential minima at the growth spirals act as emissive exciton localization centers in Al-rich Al-GaIn/AlN QWs. This peculiar structure provides insight into achieving a higher emission efficiency in Al-rich AlGaIn QW light emitters.

The authors acknowledge Y. Akashi for his assistance with crystal growth.

- ¹ Y. Narukawa, M. Ichikawa, D. Sanga, M. Sano, and T. Mukai, *J. Phys. D: Appl. Phys.* **43**, 354002 (2010).
- ² S. Keller, U. K. Mishra, S. P. DenBaars, and W. Seifert, *Jpn. J. Appl. Phys.* **37**, L431 (1998).
- ³ T. Sugahara, M. Hao, T. Wang, D. Nakagawa, Y. Naoi, K. Nishino, and S. Sakai, *Jpn. J. Appl. Phys.* **37**, L1195 (1998).
- ⁴ D. Cherns, S. J. Henley, and F. A. Ponce, *Appl. Phys. Lett.* **78**, 2691 (2001).
- ⁵ T. Miyajima, T. Hino, S. Tomiya, K. Yanashima, H. Nakajima, T. Araki, Y. Nanishi, A. Satake, Y. Masumoto, K. Akimoto, T. Kobayashi, and M. Ikeda, *Phys. Stat. Sol. (b)* **228**, 395 (2001).
- ⁶ A. Hangleiter, F. Hitzel, C. Netzel, D. Fuhrmann, U. Rossow, G. Ade, and P. Hinze, *Phys. Rev. Lett.* **95**, 127402 (2005).
- ⁷ S. Sonderegger, E. Feltn, M. Merano, A. Crottini, J. F. Carlin, R. Sachot, B. Deveaud, N. Granjean, and J. D. Ganière, *Appl. Phys. Lett.* **89**, 232109 (2006).
- ⁸ A. Kaneta, M. Funato, and Y. Kawakami, *Phys. Rev. B* **78**, 125317 (2008).
- ⁹ U. Jahn, O. Brandt, E. Luna, X. Sun, H. Wang, D. S. Jiang, L. F. Bian, and H. Yang, *Phys. Rev. B* **81**, 125314 (2010).
- ¹⁰ W. K. Burton, N. Cabrera, and F. C. Frank, *Philos. Trans. Royal Soc. London, Ser. A* **243**, 299 (1951).
- ¹¹ M. Matsubara, J. Godet, L. Pizzagalli, and E. Bellotti, *Appl. Phys. Lett.* **103**, 262107 (2013).
- ¹² B. N. Pantha, R. Dahal, M. L. Nakarmi, N. Nepal, J. Li, J. Y. Lin, H. X. Jiang, Q. S. Paduano, and D. David, *Appl. Phys. Lett.* **90**, 241101 (2007).
- ¹³ H. Hirayama, T. Yatabe, T. Ohashi, and N. Kamata, *Phys. Stat. Sol. (c)* **5**, 2283 (2008).
- ¹⁴ R. G. Banal, Y. Akashi, K. Matsuda, Y. Hayashi, M. Funato, and Y. Kawakami, *Jpn. J. Appl. Phys.* **52**, 08JB21 (2013).
- ¹⁵ A. R. Smith, V. Ramachandran, R. M. Feenstra, D. W. Greve, M.-S. Shin, and M. Skowronski, *J. Vac. Sci. Technol. A* **16**, 1641 (1998).
- ¹⁶ T. Akasaka, Y. Kobayashi, and M. Kasu, *Appl. Phys. Exp.* **3**, 075602 (2010).
- ¹⁷ C.-H. Lin, T. Akasaka, and H. Yamamoto, *Appl. Phys. Exp.* **6**, 035503 (2013).
- ¹⁸ K. Tadatomo, H. Okagawa, Y. Ohuchi, T. Tsunekawa, Y. Imada, M. Kato, and T. Taguchi, *Jpn. J. Appl. Phys.* **40**, L583 (2001).

117115-6 Funato, Banal, and Kawakami

AIP Advances **5**, 117115 (2015)

- ¹⁹ M. Funato, T. Kondou, K. Hayashi, S. Nishiura, M. Ueda, Y. Kawakami, Y. Narukawa, and T. Mukai, [Appl. Phys. Exp.](#) **1**, 011106 (2008).
- ²⁰ Y. Kawakami, A. Kaneta, L. Su, Y. Zhu, K. Okamoto, M. Funato, A. Kikuchi, and K. Kishino, [J. Appl. Phys.](#) **107**, 023522 (2010).
- ²¹ H. K. Cho, J. Y. Lee, and G. M. Yang, [Appl. Phys. Lett.](#) **80**, 1370 (2002).
- ²² D. Fuhrmann, T. Retzlaff, M. Greve, L. Hoffmann, H. Bremers, U. Rossow, A. Hangleiter, P. Hinze, and G. Ade, [Phys. Rev. B](#) **79**, 073303 (2009).
- ²³ A. Petersson, A. Gustafsson, L. Samuelson, S. Tanaka, and T. Aoyagi, *MRS Internet J. Nitride Semicond. Res.* **7**, e5 (2002).
- ²⁴ A. Pinos, V. Liuolia, S. Marcinkevičius, J. Yang, R. Gaska, and M. S. Shur, [J. Appl. Phys.](#) **109**, 113516 (2011).
- ²⁵ Z. Sitar, B. Moody, S. Craft, R. Schlessler, R. Dalmau, J. Xie, S. Mita, T. Rice, J. Tweedy, J. LeBeau, L. Hussey, R. Collazo, B. Gaddy, and D. Irving, in *Int. Workshop on Nitride Semicond.*, 2012, pp. S3-4.
- ²⁶ M. Funato, Y. Hayashi, and Y. Kawakami, [J. Appl. Phys.](#) **115**, 103518 (2014).